Isothermal and Non-Isothermal Consolidation of Carbon Fiber Towpregs

J. P. NUNES, A. M. BRITO, A. S. POUZADA, *and* C. A. BERNARDO

Department of Polymer Engineering
Universidade do Minho
4800-058 Guimarães, Portugal

The purpose of this work is to establish and validate a model to predict the isothermal and non-isothermal consolidation behavior of unidirectional towpregs, made of carbon fibers and a thermoplastic polymer. A Finite Difference Method program was devised based on a set of analytical expressions developed in a previous work. The program allows the determination of pressure-displacement curves at constant press closing speed and fixed or variable molding temperature, allowing comparison with experimental data obtained in the same conditions. There was good agreement between theoretical predictions and experimental results for both the isothermal and non-isothermal consolidation. However, in the former case, the agreement was limited to low closing speeds and long pre-heating times. In the latter case these limitations did not exist, showing that the non-isothermal model is a good tool for the optimization of the consolidation process.

INTRODUCTION

There has been a consistent trend in recent years to develop the technology of long fiber composites with thermoplastic matrices, either to facilitate their processing or to obtain better performing parts (1, 2). The ultimate goal is to replace thermoset-based composites in high-volume applications. There are various practical reasons for that, the major one being the possibility of recycling the used materials. The initial difficulties, arising from the high cost and environmental impact of the process, could be overcome by using a technique of powder coating continuous fibers (2–8). The resulting prepregs, known as towpregs, as they are fiber tows pre-impregnated with small thermoplastic particles, can be easily processed by compression molding.

Adequate properties, namely mechanical properties, are another important requirement of a consolidated towpreg. This can be achieved by selecting high performance materials, adequate control of the compression conditions or both. Using carbon fibers as reinforcements, towpreg laminates could be consolidated into composites with superior mechanical properties (8). It was found that compression molding was a critical step to obtain those properties. Therefore, it should be well understood. However, only preliminary descriptions of this step seem to have been published (9, 10). Thus, it was found necessary to gather more experimental data on the compression molding of towpregs, and develop a theory to predict the behavior of the material as it consolidates. Such an experimental and theoretical investigation has just been reported (11, 12). In that work, a predictive model for the evolution of the pressure during the compression molding of a polycarbonate/PAN-based carbon fiber towpreg was derived and validated. The model considers that the instantaneous pressure applied to the material is a function of its characteristics (viscosity, fiber and polymer particle size and polymer volume fraction), and the consolidation conditions (press closing speed and mold temperature).

In spite of the normally good agreement between theory and experimental results, deviations were sometimes observed. They mostly derived from the assumptions upon which the model was based. Possibly the most stringent one was to consider the consolidation as an isothermal process. Although "isothermal" consolidations are often used in industrial practice, the constancy of the temperature is far from certain, especially in the inner laminae of the consolidate. Thus, it is necessary to consider a more general model, that takes into account the evolution of temperature through the material thickness. The present work reports the derivation of one such model, based on a Finite Differences Method (FDM). The model is able to predict, from the thermal properties of the material and the initial temperature, the variation of the temperature with the distance from the mold platens and with time. It also considers different arrangements for the towpreg lamina stacks that are formed

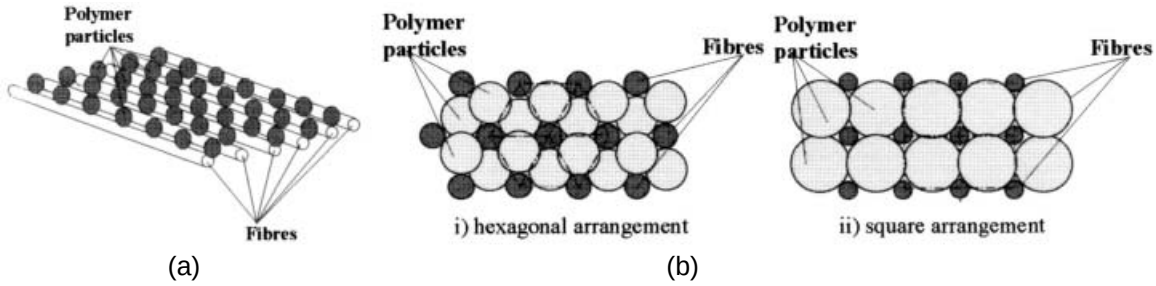

Fig. 1. Geometry of a towpreg laminate: a) towpreg lamina; b) different arrangements of the laminae stacking.

into composites. The model predictions were compared with experimental data obtained with the towpreg already used in the previous work (11, 12).

THEORY

A towpreg can be envisaged as an array of fibers with particles attached forming a lamina (*Fig. 1a*). Stacking a number of these laminae together with different possible arrangements leads to a preform (*Fig. 1b*). The preforms are normally processed by compression molding to produce a composite. As stated above, a model has already been derived to describe this process in isothermal conditions. Consequently, only its main aspects will be briefly reviewed in this section. The derivation of the isothermal model was based upon the following assumptions:

i) the fibers and the polymer are at constant temperature during the processing;

ii) the polymer and the fibers are incompressible;

iii) upon compression, the bridges spread in the direction of the fibers and the pressure is considered constant through thickness;

iv) the press closing speed is constant;

v) no voids are left after consolidation;

vi) the polymer flow is laminar and steady, and inertial forces are negligible.

In this model it was assumed that during consolidation each polymer particle forms a bridge between three adjacent fibers (*Fig. 2a*). The rationale behind this hypothesis was that this hexagonal arrangement, that corresponds to the natural close packing of circular fibers, supposedly leads to better results. In the present derivation the square arrangement (*Fig. 2b*), which implies a looser packing, will also be considered.

To model the consolidation stage, the final and the instantaneous bridge lengths must be related to the volume fraction of fibers, the composite thickness and the initial dimensions of the polymer particles.

As the traverse dimension of the laminate remains constant during consolidation, the rate of decrease of its instantaneous thickness, $\dot{h}(t)$, coincides with the press closing speed, s_p (see *Fig. 3*). Then, it is possible to relate these variables with the platen displacement, Δ, and the initial thickness, h_0, by:

$$\Delta = h_0 - h(t) \rightarrow \frac{d\,\Delta(t)}{dt} = -\frac{dh(t)}{dt} = s_p \qquad (1)$$

At any time during consolidation, the fiber, matrix and void volume contents, v_f, v_p and v_v, are related by:

$$v_f + v_p + v_v = 1 \qquad (2)$$

When the press displacement stops no voids are left, but the volume of the polymer (and that of the

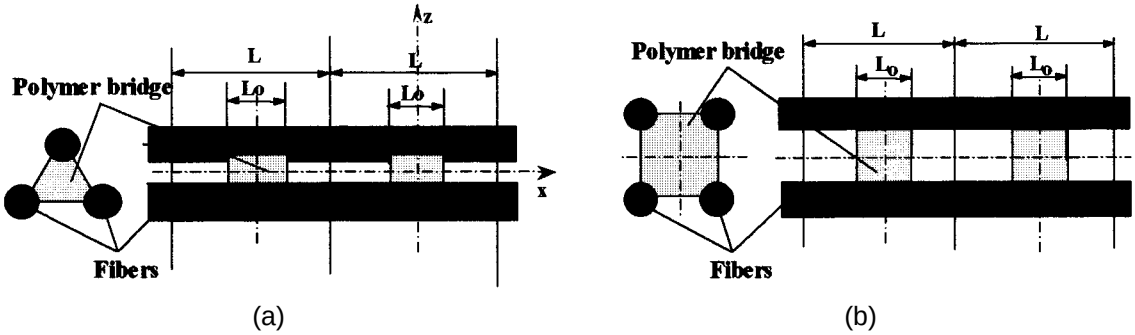

Fig. 2. Schematic representation of the polymer bridge at the beginning of the consolidation: a) hexagonal arrangement; b) square arrangement. L_0 and L are the initial and final polymer bridge lengths, respectively.

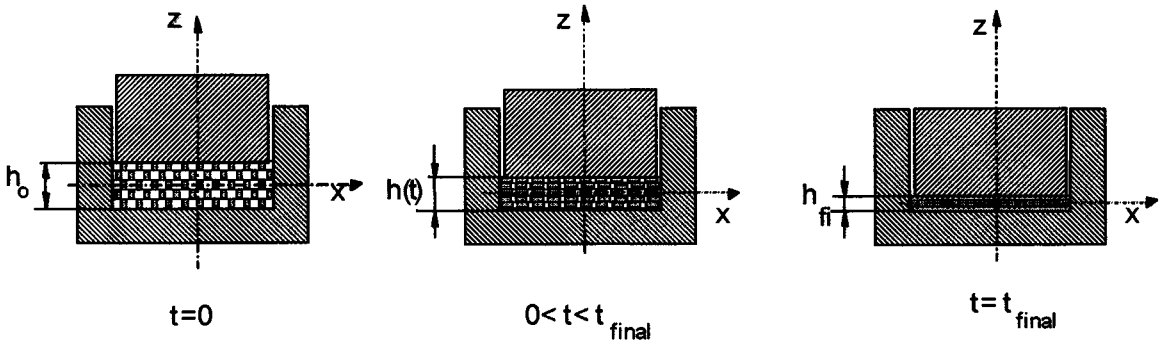

Fig. 3. Evolution of the molding geometry during the compression of a towpreg.

fibers) is the same as at the beginning. Then, it is possible to relate those variables with the composite thickness, h(t), by:

$$v_f = \frac{h_{fi} v_{fi}}{h(t)};\quad v_p = \frac{h_{fi}(1 - v_{fi})}{h(t)};\quad v_v = \frac{h(t) - h_{fi}}{h(t)} \qquad (3)$$

where h_{fi} and v_{fi} are the final thickness of the molding and the final fiber volume fraction, respectively.

In the hexagonal and square fiber/polymer arrangements each bridge links three and four fibers, and is shared by six and four closest neighbors, respectively. Then, considering one single bridge, the fiber volume fraction can be calculated as:

$$\text{hexagonal arrangement: } v_f = \frac{3\frac{\pi}{6}(r_f)^2 L}{3\frac{\pi}{6}(r_f)^2 L + \frac{4}{3}\pi(r_p)^3}$$

$$\text{square arrangement: } v_f = \frac{4\frac{\pi}{6}(r_f)^2 L}{4\frac{\pi}{6}(r_f)^2 L + \frac{4}{3}\pi(r_p)^3} \qquad (4)$$

where r_p and r_f are the initial radii of the polymer particle and fiber, respectively, and L is the final polymer bridge length.

Then, solving *Eq 4* in order to L, and considering that, at the end of the compression, $v_f = v_{fi}$, the final bridge length will be given by:

$$\text{hexagonal arrangement: } L = \frac{8}{3}\frac{(r_p)^3}{(r_f)^2}\left(\frac{v_{fi}}{1 - v_{fi}}\right)$$

$$\text{square arrangement: } L = \frac{4}{3}\frac{(r_p)^3}{(r_f)^2}\left(\frac{v_{fi}}{1 - v_{fi}}\right) \qquad (5)$$

Identically, the instantaneous polymer bridge length, L(t), can be calculated as

$$\text{hexagonal arrangement: } L(t) = \frac{8}{3}\frac{(r_p)^3}{(r_f)^2}\left(\frac{v_f}{1 - v_f}\right)$$

$$\text{square arrangement: } L(t) = \frac{4}{3}\frac{(r_p)^3}{(r_f)^2}\left(\frac{v_f}{1 - v_f}\right) \qquad (6)$$

Then, replacing v_f in *Eq 6* by its value given by *Eq 3*, leads to:

$$\text{hexagonal arrangement: } L(t) = \frac{8(r_p)^3 h_{fi} v_{fi}}{3(r_f)^2 h(t)\left(1 - \frac{h_{fi} v_{fi}}{h(t)}\right)}$$

$$\text{square arrangement: } L(t) = \frac{4(r_p)^3 h_{fi} v_{fi}}{3(r_f)^2 h(t)\left(1 - \frac{h_{fi} v_{fi}}{h(t)}\right)} \qquad (7)$$

The derivation continues by calculating the pressure gradient, $\frac{dp}{dx}$, required to cause the flow of the polymer particle in the fiber direction. From $\frac{dp}{dx}$ it is possible to obtain an expression relating the viscous pressure to the properties of the towpreg and the press closing speed. As shown previously for the isothermal model and hexagonal arrangement (11–14), this can be done by applying the continuity, Darcy and Carman-Kozeny equations to calculate the average polymer velocity. The derivation is formally the same for the hexagonal and square arrangements, being only necessary to use the correct expressions of v_f, L and L(t), as given by *Eqs 4*, *5* and *7*, respectively. Consequently, it will not be repeated here. The value of the viscous pressure thus obtained is:

$$p = -\frac{C\,\dot{h}(t)}{[h(t) - h_{fi} v_{fi}]^6} \qquad (8)$$

In the above equation, C is a constant that depends on the towpreg properties, the press operation and the fiber/polymer arrangement. For hexagonal and square packing the values of C are, respectively:

$$C = \frac{64\eta s_p k_{xx}(h_{fi})^5 (v_{fi})^4 (1 - v_{fi})(r_p)^6}{27(r_f)^6}$$

$$C = \frac{16\eta s_p k_{xx}(h_{fi})^5 (v_{fi})^4 (1 - v_{fi})(r_p)^6}{9(r_f)^6} \qquad (9)$$

where η is the polymer viscosity, r_f and r_p are the fiber and polymer particle radii; k_{xx} is the Carman-Kozeny constant, which can be considered equal to 0.7 according to Gutowski *et al.* (13).

As will be shown later, for the utilization of the model it is also necessary to consider the instantaneous shear rate, $\dot{\gamma}$, of the molten polymer through the fiber interstices. This shear rate is related to the characteristics of the material and the consolidation conditions. As shown elsewhere (11, 12, 15), the maximum value of $\dot{\gamma}$ for the hexagonal and square arrangements is:

$$\dot{\gamma}(x) = \frac{4k_{xx}}{r_f}\frac{v_f}{(1-v_f)^2}\frac{x}{h(t)}\frac{dh(t)}{dt} \tag{10}$$

Then, considering *Eqs 1*, *3* and *7*, the final expressions for the maximum instantaneous shear rates can be obtained:

hexagonal arrangement:

$$\dot{\gamma}_{max} = \frac{16\, s_p k_{xx} (r_p)^3 (h_{fi}\, v_{fi})^2}{3(r_f)^3\, h(t)^3 \left(1 - \dfrac{h_{fi} v_{fi}}{h(t)}\right)^3}$$

square arrangement:

$$\dot{\gamma}_{max} = \frac{8\, s_p k_{xx} (r_p)^3 (h_{fi}\, v_{fi})^2}{3(r_f)^3\, h(t)^3 \left(1 - \dfrac{h_{fi} v_{fi}}{h(t)}\right)^3} \tag{11}$$

As can be seen from *Eqs 8* and *9*, the pressure necessary to consolidate a towpreg with a hexagonal fiber/polymer arrangement is approximately 4/3 of that for a square arrangement. Also, as shown by *Eq 11*, a double shear rate is obtained for the flow of the molten polymer through the fiber interstices in the former case.

At this stage, using the viscosity, it is possible to express the dependence of the pressure on the temperature through *Eqs 8* and *9*. This will then allow the consideration of the two different procedures, the isothermal and non-isothermal consolidation.

Isothermal Consolidation

When the consolidation is isothermal, all composite layers are at the mold temperature. Then, as the above derivation shows, the instantaneous pressure can be analytically determined if the fiber and particle polymer radii, the final molding thickness and fiber volume fraction are known.

An Arrhenius power law is used to relate the polymer viscosity, η, at each mold temperature:

$$\eta = m_o\, e^{\left(\frac{\Delta E}{RT}\right)} \times (\dot{\gamma})^{n-1} \tag{12}$$

where T is the mold absolute temperature and R the gas constant. The polymer consistency when T approaches infinity, m_o (Pa.s^n), the polymer flow activation energy, ΔE, and the shear rate, can be determined experimentally.

Then, for different temperatures and shear rates and for the two arrangements, the final expressions of the constant C in *Eq 8* are:

hexagonal arrangement:

$$C = m_o e^{\left(\frac{\Delta E}{RT}\right)} \times (\dot{\gamma})^{n-1}\, \frac{64 s_p k_{xx} (h_{fi})^5 (v_{fi})^4 (1 - v_{fi})\, (r_p)^6}{27 (r_f)^6}$$

square arrangement:

$$C = m_o e^{\left(\frac{\Delta E}{RT}\right)} \times (\dot{\gamma})^{n-1}\, \frac{16 s_p k_{xx} (h_{fi})^5 (v_{fi})^4 (1 - v_{fi})\, (r_p)^6}{9 (r_f)^6} \tag{13}$$

By introducing in *Eq 13* the value of $\dot{\gamma}$ as given by *Eq 11*, a final expression to model the evolution of the viscous pressure during the isothermal consolidation can be obtained.

Non-Isothermal Consolidation

In non-isothermal conditions, the temperature varies through the thickness of the towpreg. As the polymer viscosity depends on temperature, the material layers deform at different rates. Thus, to calculate the instantaneous pressure it is necessary to determine numerically the temperature gradient along the laminate z co-ordinate axis (*Fig. 4*).

Considering as negligible the generation and transfer of heat by viscous dissipation and convection, the instantaneous temperature at a point of co-ordinate z is calculated using finite differences, to solve the simplified equation of energy:

$$\frac{\partial T}{\partial t} = \alpha \frac{\partial^2 T}{\partial z^2} \tag{14}$$

where α is the thermal diffusivity,

$$\alpha = \frac{k}{\rho C_p} \tag{15}$$

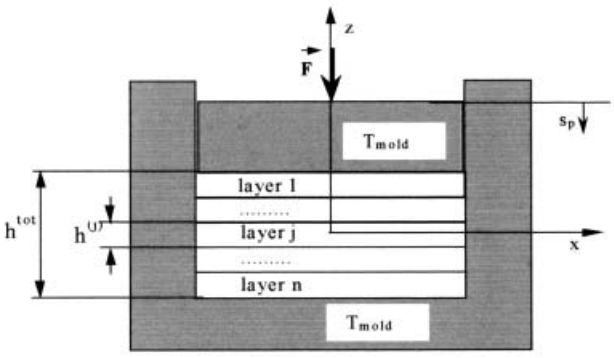

Fig.4. Scheme of a towpreg laminate used in the non-isothermal model.

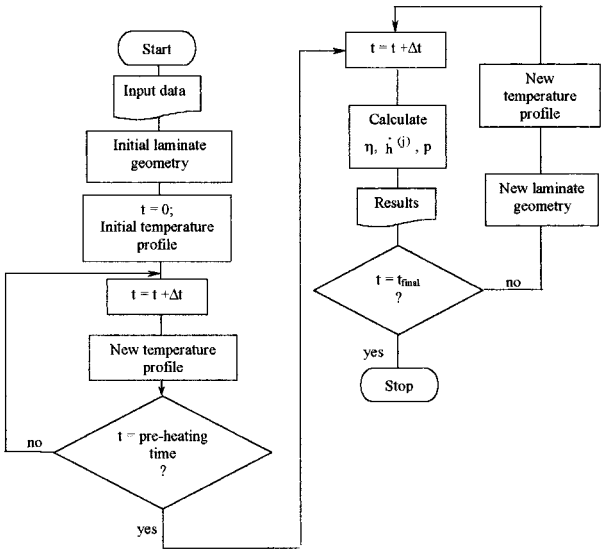

Fig. 5. Non-isothermal simulation flowchart.

In the above equation, k is the thermal conductivity, C_p is the specific heat and ρ is the density of the material.

The following boundary conditions are considered (*Fig. 4*):

$T_{mold} = constant$ and

$$\text{at } z = \pm\frac{h^{tot}}{2},\ T = T_{mold} \tag{16}$$

where h_o^{tot} is the laminate initial thickness.

Figure 5 shows the flowchart used in the program that simulates the non-isothermal consolidation performed at constant press closing speed. As the *Figure* suggests, the determination of the temperature gradient is made in two steps using small increments of time (Δt). In a first step, the composite, consisting of layers of equal thickness, is pre-heated without pressure, and the temperature field through the thickness is calculated. In a second step, the layers are considered to have different rheological and thermal properties, and to deform at different rates.

The total number of layers, n, and the initial and final thickness of layer j, $h_o^{(j)}$ and $h_{fi}^{(j)}$, were determined by:

$$h_{fi}^{(j)} = r_f\sqrt{\frac{\pi\sqrt{3}}{2v_{fi}}} \tag{17}$$

$$h_o^{(j)} = \frac{3}{2}(r_f + r_p) \tag{18}$$

$$n = integer\left(\frac{h_{fi}^{tot} - 2r_f}{h_{fi}^{(j)}}\right) \tag{19}$$

$$h_o^{tot} = n \times h_o^{(j)} + 2r_f \tag{20}$$

At each instant, t_i, during compression, the polymer viscosity is determined at each layer, using *Eq 12* and the temperature calculated at its middle-plan. Thus, considering the pressure constant through thickness and using *Eqs 8* and *9*, the instantaneous deformation rate of each layer j, $\dot{h}^{(j)}$, is calculated by solving the system of n equations:

$$\dot{h}^{(j)} = \frac{\eta^{(j+1)}\left[h^{(j)} - h_{fi}v_{fi}\right]^6}{\eta^{(j)}\left[h^{(j+1)} - h_{fi}v_{fi}\right]^6}\cdot\dot{h}^{(j+1)} \qquad j = 1, \ldots, n-1$$

$$\sum_{j=1}^{n}\dot{h}^{(j)} = s_p \tag{21}$$

where the closing speed is considered to be equal to the sum of the deformation rates of all layers, and $\eta^{(j)}$ and $h^{(j)}$ are the instantaneous viscosity and thickness of the layer j.

From the layer deformation rate, $\dot{h}^{(j)}$, the position of the layers in the z-axis needs to be determined for the next instant, $t_{i+1} = t_i + \Delta t$. The conductivity of each layer j, $k^{(j)}$, is then calculated as:

$$\frac{1}{k^{(j)}} = \frac{v_f^{(j)}}{k_f} + \frac{v_p^{(j)}}{k_p} + \frac{v_v^{(j)}}{k_v} \tag{22}$$

where k_f, k_p, k_v are the conductivities of the fiber, polymer and air, respectively and $v_f^{(j)}$, $v_p^{(j)}$, $v_v^{(j)}$ are their volume fractions in layer j. At each layer, *Eq 3* is used to determine the volume fraction of the components.

On the other hand, the specific heat of each layer, $C_p^{(j)}$, is given by

$$C_p^{(j)} = C_{pf}\,w_f^{(j)} + C_{pp}\,w_p^{(j)} + C_{pv}\,w_v^{(j)} \tag{23}$$

where C_{pf}, C_{pp} and C_{pv} are the specific heats of the fiber, polymer and air respectively, and $w_f^{(j)}$, $w_p^{(j)}$, $w_v^{(j)}$ their mass fractions in layer j.

EXPERIMENTAL WORK

Characterization of Materials

A polycarbonate powder (Bayer Makrolon 2458) and high strength PAN carbon fibers (Amoco Thornel T300/12/NT) were used to produce towpregs in the dry powder coating unit described in a previous work (3, 8, 12). The dimension and size distributions of the polycarbonate powder were determined using image analysis and sieving techniques. The irregularly shaped powder particles had an average diameter of 156 μm.

The viscosity of the polymer was measured at low shear rates with a TA Instruments Weissenberg rheogoniometer. The data, determined at four temperatures (220, 240, 260 and 280°C) and shear rates up to 10 s^{-1}, were used to calculate the parameters of *Eq 12*.

The average diameter of the PAN carbon fibers, determined by a laser diffraction technique, was 7.2 μm. The fiber volume fraction was calculated as 25.3 ± 2.04%.

Table 1. Typical Processing Conditions for the Consolidation of the Laminates.

Property	Units	Sample Reference			
		A	B	C	D
Temperature (T)	°C	220	240	260	280
Press closing speed (s_p)	$mm.s^{-1}$	0.035	0.045	0.05	0.10
Viscosity (η)	Pa · s	8810	2460	1000	570
Average shear rate ($\dot{\gamma}$)	s^{-1}	55	60	72	120

Consolidation Tests

An instrumented 800 kN SATIM press with two independently heated plates was used to produce laminates at temperatures from 220 to 280°C. The pressure and platen displacement were continuously monitored and recorded in a x-t recorder. The towpreg laminate was pre-heated in the mold for 10 min. The consolidation conditions are summarized in *Table 1*.

RESULTS AND DISCUSSION

Isothermal Consolidation

Figure 6 compares the experimental values of the applied pressure, normalized with the closing speed and the viscosity of the material, with the simulation results, for both the hexagonal and square fiber/polymer arrangements. Visual inspection of the *Figure* shows that the fitting is quite good for both cases. However, in the last stages of compression, the hexagonal model seems to fit the data better. This may suggest that the hexagonal arrangement is closer to the actual packing that the fibers assume during the consolidation.

In spite of the good fitting, the isothermal simulations provide little information about the influence of the pre-heating time and the closing speed. For example, when the pre-heating times were lower than 10 minutes, experimental pressures greater than expected were obtained in the beginning of compression. This situation certainly derives from the low temperature in the internal layers of the laminate and the resulting increase in viscosity. The same situation occurred when the press closing speed increased. In this case, the higher pressures are developed due to the slow heat transfer that prevents the material internal layers of reaching the set temperature.

Non-Isothermal Consolidation

The evolution of the temperature across thickness during the consolidation of the carbon/polycarbonate towpreg for three different pre-heating times (5, 10 and 20 min) is shown in *Fig. 7*. The plots were calculated considering towpreg and mold initial temperatures of 25°C and 260°C, respectively, and the material properties shown in *Table 2*.

As shown in *Fig. 7*, the temperature amplitude in the molding depends strongly on the pre-heating time. For short pre-heating times, the temperature difference can be over 100°C in the early compression stages. For these towpregs it is necessary to pre-heat for 20 minutes to reach a quasi-constant temperature through thickness. If 5 minutes were used instead, the polycarbonate at the center of the laminate remained solid during most of the compression. The criterion for ascertaining the pre-heating time can be linked with the no-flow temperature of polycarbonate that is typically of the order of 200°C (16). With this datum, the minimum recommended pre-heating time

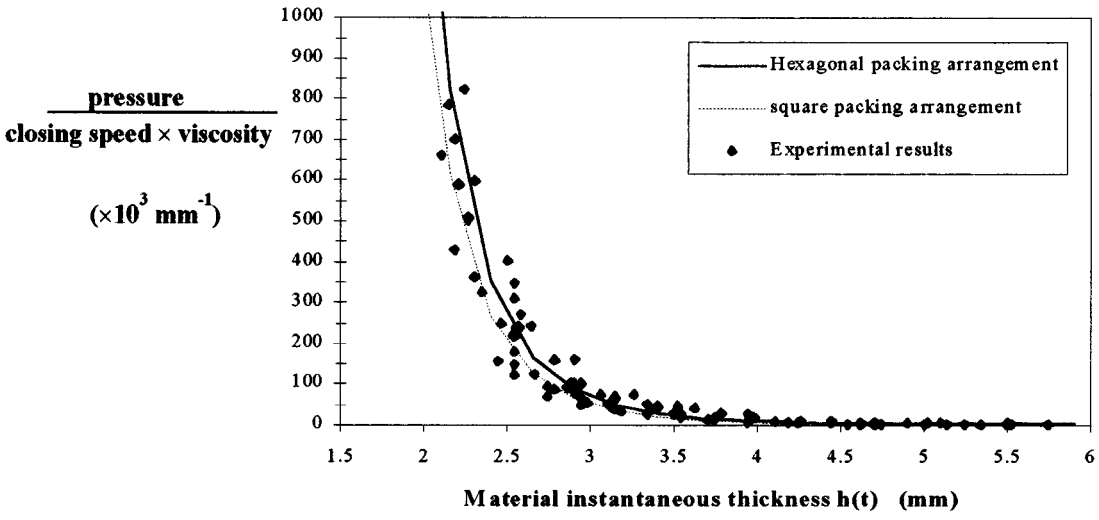

Fig. 6. Experimental and theoretical pressure data as a function of the material instantaneous thickness.

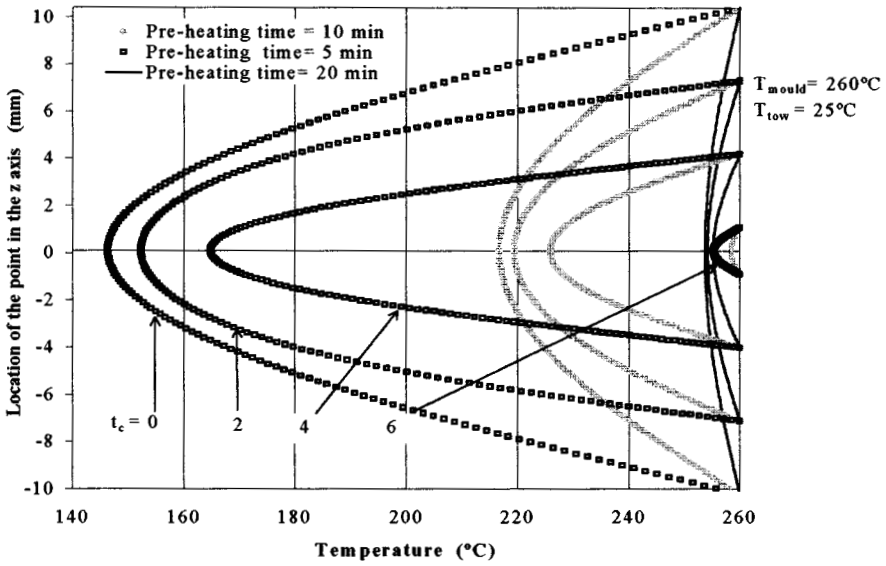

Fig. 7. Variation of the temperature across thickness for different pre-heating times at various compression times (t_c = 0, 2, 4 and 6 min).

can be derived graphically, as shown in *Fig. 8*, where the temperature amplitude at z = 0, with t_c = 0, is plotted against the pre-heating time. The recommended time is obtained by the intersection of the curve and the temperature amplitude corresponding to the difference between the no-flow and the mold temperatures. If the compression starts before this time, some layers will not flow. This explains the discrepancies observed between the theory and the experimental data for the isothermal consolidation with short pre-heating times.

In *Fig. 9*, pressure data obtained from consolidation tests at 260°C are compared with simulations for the isothermal and non-isothermal models using a pre-heating time of 10 min hexagonal packing and two different closing speeds. It is apparent that the predictions of non-isothermal model are closer to the experimental results, namely in the beginning of compression. The worst fitting is obtained for the isothermal simulation at the higher closing speed.

The deformation rates of the different layers are represented as a function of the compression time for a laminate with 168 layers in *Fig. 10*. It is evident that, at the beginning of the compression, the layers in contact with the mold (layer 1 and also layer 168, not shown due to the symmetry) decrease in thickness more rapidly than the middle-plan layer (layer 84). Layer 42 will represent an intermediate situation. However, as the top and bottom layers also suffer a quicker thickness reduction, they become progressively more difficult to deform. This explains the tendency for all layers to display similar deformation rates as the compression progresses, in spite of the large through-thickness temperature differences shown in *Fig. 7*.

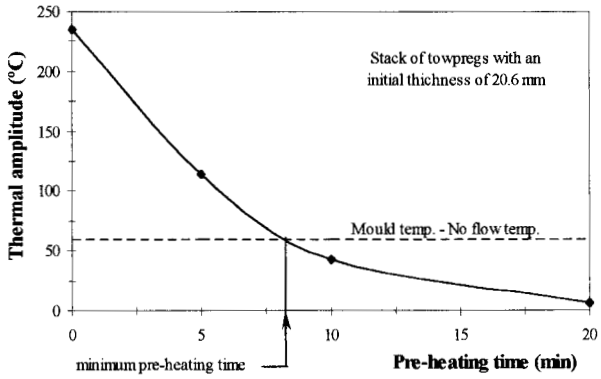

Fig. 8. Calculation of the pre-heating time necessary for towpreg flow.

Table 2. Values of the Properties Used in the Simulations.

	Thermal Conductivity (W/m.K)	Density (kg/m^3)	Specific Heat (kJ/kg·K)	Radius (μm)
Fiber	8.5	1760	0.925	3.6
Polymer	0.25	1200	1.8	78
Air	0.025	1.1	1.005	—

v_{fi} = 25%, h_{fi}^{tot} = 2 mm, s_p = 0.05 mm/s, m_o = 46.3 nPa.s^n, $\frac{\Delta E}{R}$ = 12860 K, n = 0.953

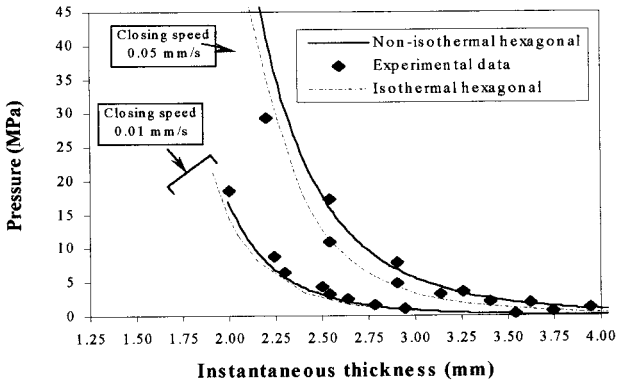

Fig. 9. Comparison between the experimental data and the isothermal and non-isothermal simulations at 260°C.

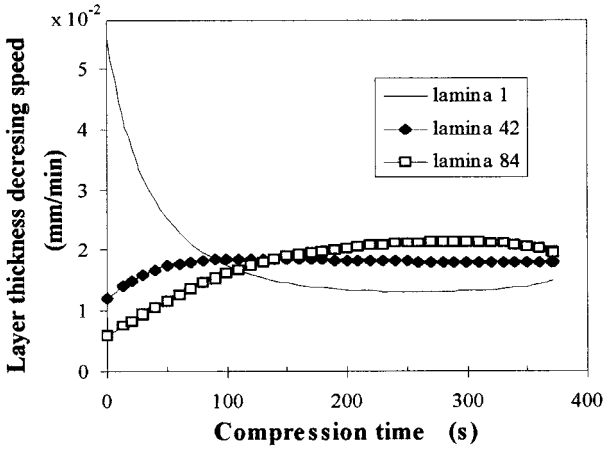

Fig. 10. Comparison between the deformation rates of different laminate layers during the consolidation at 260°C using a pre-heating time of 10 minutes.

An attempt was made to use the FDM program developed in this work to simulate the towpreg consolidation in the cooling mode. This alternative mode has a real practical importance. In fact, in industrial conditions, the compression of pre-heated towpregs in a cold mold would reduce the processing cycle considerably, by eliminating the mold-cooling phase. However, the simulation results showed that it was necessary to use quite high compression rates (similar to those used in stamping) to achieve adequate consolidation in a cold mold. These high rates are not compatible with the basic assumptions of the model, namely the consideration of laminar and steady flow of the molten polymer through the fibers' interstices. As a consequence, the derivation of a new model will have to be made in the future to simulate the consolidation of towpregs in the cooling mode.

CONCLUSIONS

A model to simulate the consolidation of powder coated towpregs in isothermal and non-isothermal conditions was developed in this work. The fitting of the theoretical expressions developed for the hexagonal and square arrangements supports the view that the fibers assume the hexagonal close packing during consolidation. The results also show that the model can only predict successfully the consolidation in isothermal conditions if a minimum pre-heating time and low press closing speeds are used. Globally, it was concluded that the non-isothermal predictions fit better the experimental data. Therefore, the optimization of the consolidation rate by fine-tuning of the pre-heating time must be based on a non-isothermal model.

The attempts to use the model developed in this work to describe the consolidation of towpregs in the cooling mode were not successful. The simulations suggested that, in this mode, the press closing speeds necessary for a proper consolidation are so high that the model no longer applies. A new model is thus necessary to simulate this situation of clear practical importance.

ACKNOWLEDGMENTS

The support of the Institute of Materials (IMAT) and of the Center for Polymer Engineering of the Universidade do Minho to the present work is gratefully acknowledged. Thanks are also due to the Fundação Luso-Americana para o Desenvolvimento (FLAD) for financing the mobility of the researchers involved in the project.

NOMENCLATURE

C	constant in *Eq 8*
C_p	specific heat of the material
C_{pf}	specific heat of the fibers
C_{pp}	specific heat of the polymer
C_{pv}	specific heat of air
h_0	initial composite thickness
h(t)	instantaneous composite thickness
h_{fi}	final composite thickness
$\dot{h}(t)$	rate at which the molding thickness decreases
h_o^{tot}	laminate initial thickness in the non-isothermal simulation
$h_o^{(j)}$	initial thickness of layer j
$h_{fi}^{(j)}$	final thickness of layer j
j	counter of the layers in the non-isothermal simulation
k	thermal conductivity of the material
k_f	thermal conductivity of the fibers
k_p	thermal conductivity of the polymer
k_v	thermal conductivity of air
k_{xx}	Carman-Kozeny constant (in the fiber direction) ≈ 0.7
L_o	initial polymer bridge length
L(t)	instantaneous polymer bridge length
L	final polymer bridge length
m_o	polymer consistency index when the temperature approaches infinity
n	number of laminate layers in the non-isothermal simulation

- p applied pressure
- r_p initial radius of the polymer particle
- r_f radius of the fiber
- s_p closing speed of the mold (constant)
- T absolute temperature
- v_f instantaneous volume fraction of fibers
- $\dot{v}_f$ rate of variation of the volume fraction of fibers
- v_{fi} final volume fraction of fibers
- v_p instantaneous volume fraction of polymer
- v_v instantaneous volume fraction of voids
- z co-ordinate axis
- $w_f^{(j)}$ mass fraction of fibers in layer j
- $w_p^{(j)}$ mass fraction of polymer in layer j
- $w_v^{(j)}$ mass fraction of air in layer j
- α thermal diffusivity of the material
- $\dot{\gamma}_w$ shear rate associated with the flow of the polymer in the fibers' interstices
- Δ platen displacement
- ΔE activation energy for polymer flow
- η polymer viscosity
- ρ polymer density

REFERENCES

1. J. Brandt, K. Drechsler, and H. Richter, in *Proc. ICCM-9 Conf.*, Vol. VI, 143, Madrid (1993).
2. J. T. Hartness, *J. Thermoplastic Composite Materials*, **1**, 210 (1988).
3. B. W Gant, D. D Edie, G. C. Lickfield, M. J. Drews, and M. S. Ellison, in *Proc ASTM STP 1004*, p. 50, G. M. Newaz, ed., Philadelphia (1989).
4. S. R. Iyer and L. T. Drzal, *J. Thermoplastic Composite Materials*, **3** (4), 325 (1990).
5. A. Miller, C. Wei, and A. G. Gibson, *Composites Part A*, **27A** (1), 49 (1996).
6. A. G. Gibson and J. A. Manson, *Composites Manufacturing*, **3** (4), 223 (1992).
7. K. Ramani, M. Tryfonidis, C. Hoyle, and J. Gentry, in *Processing, Fabrication and Manufacturing of Composite Materials*, ASME MD, 633 (1992).
8. J. P. Nunes, C. A. Bernardo, A. S. Pouzada, and D. D. Edie, *J. Composite Materials*, **31** (17), 1758 (1997).
9. S. Padaki and L. T. Drzal., in *Proc. 9th Technical Conference of the American Society for Composites*, 1229 (1994).
10. M. Connor, A. Gibson, S. Toll, and J. A. Manson, in *Proc. ICCM-9 Conf.*, Vol. III, 332, Madrid (1993).
11. J. P. Nunes, C. A. Bernardo, A. S. Pouzada, and D. D. Edie, *Polymer Composites*, **20** (2), 260 (1999).
12. J. P. Nunes, Ph. D. Thesis, University of Minho, Portugal (1998).
13. T. G. Gutowski, Z. Cai, S. Bauer, D. Boucher, J. Kingery, and S. Wineman, *J. Composite Materials*, **21** (7), 650 (1987).
14. G. Hudgins, B. Love, and J. Muzzy, in *Proc. ICCM-9 Conf.*, Vol. II, 297, Madrid (1993).
15. Z. Tadmor and C. G. Gogos, *Principles of Polymer Processing*, John Wiley & Sons, Inc., New York (1979).
16. R. Pakull, V. Guigo, and D. Freitag, in *Polycarbonate: a RAPRA Review Report*, Report 42 (1991).